

Supporting Information

Mid-infrared High-performance Spectropolarimetry Filter Based on Dual-mode Independent Modulation

S1. Polarization properties of single-layer metal grating

As a comparison with the bi-layer grating, the transmittance and extinction ratio, as well as the electric field distribution, are given for a single-layer metal grating with the same period and layer thickness as a bi-layer metal grating. The transmittance of the single-layer metal grating is about 70% for the structural parameters of $p = 180$ nm, $w = 108$ nm, $h_m = 100$ nm. But the polarization extinction ratio is much lower than that of the double-layer metal grating, which is only a few hundred.

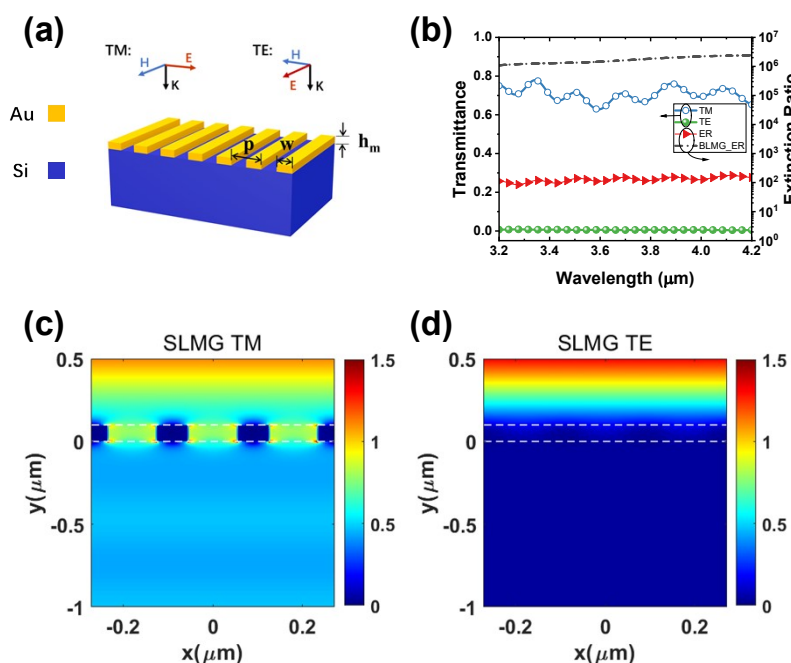


Fig.S1 (a) Schematics of single-layer metal grating (SLMG) with structure parameters $p = 180$ nm, $w = 108$ nm, $h_m = 100$ nm. (b) TM polarization (blue line) and TE polarization (green line) transmittance, SLMG extinction ratio (red line) and BLMG extinction ratio spectra (gray dotted line). (c) Electric field distribution maps under TM polarization. (d) Electric field distribution maps under TE polarization.

S2. Electric field distribution of BLMG with the different distance between the upper and lower metal grating layers.

For TM polarization, from the electric field distribution of BLMG, we find a multi-level resonant like the FP cavity, with the distance between the upper and lower metal grating layers increasing ($h_d = 0.45$ μm , 2 μm , and 3 μm) (Fig. S2). Therefore, higher TM transmittance than SLMG can be obtained at BLMG when h_d thickness meet resonance.

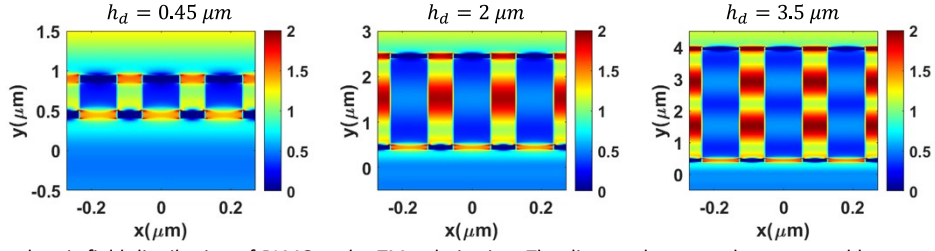


Fig.S2 The electric field distribution of BLMG under TM polarization. The distance between the upper and lower metal grating layers (a) $h_d = 0.45 \mu\text{m}$, (b) $h_d = 2 \mu\text{m}$, and (c) $h_d = 3 \mu\text{m}$.

S3. The electric field distribution map of SPF under TE polarization with enlarged FP cavity part.

The enlarged electric field distribution map of FP cavity part (Fig.S3(right)) shows that there is electric field accumulation in the FP cavity under TE polarization, but it is very weak. This causes a slight increase in TE polarization transmittance at resonance wavelength, but does not affect the polarization performance of the SPF much.

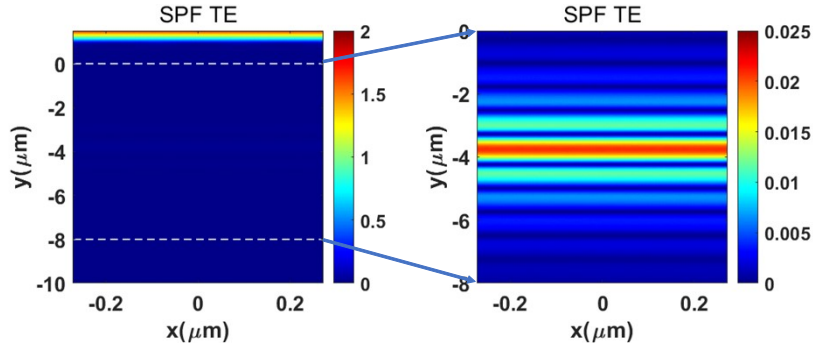


Fig.S3 The electric field distribution of SPF under TE polarization (left), and enlarged electric field distribution map of FP cavity part(right).

S4. The electric field distribution of SPF under TE polarization.

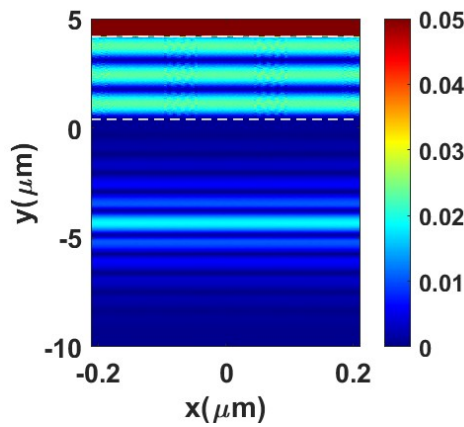


Fig.S4 The electric field distribution of SPF under TE polarization with $h_d = 3.73 \mu\text{m}$.

S5. The fabrication process of SPF.

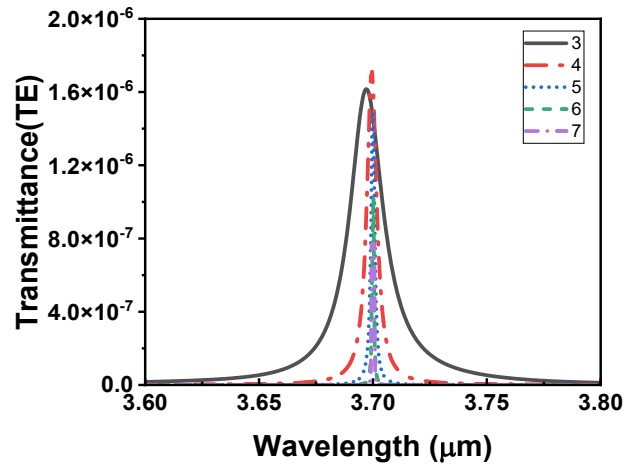


Fig.S5 The TE transmittance of SPF with different pair number m.

S6. The fabrication process of SPF.

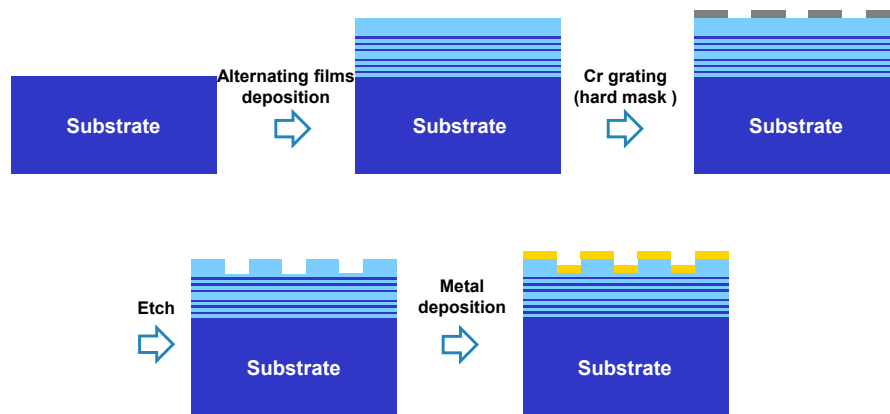


Fig.S6 The fabrication process of SPF.

S7. Absorption spectra of striated muscle and rhabdomyosarcoma tissue under unpolarized conditions.

In non-polarized mode, striated muscle and rhabdomyosarcoma tissue exhibit similar spectral absorption characteristics.

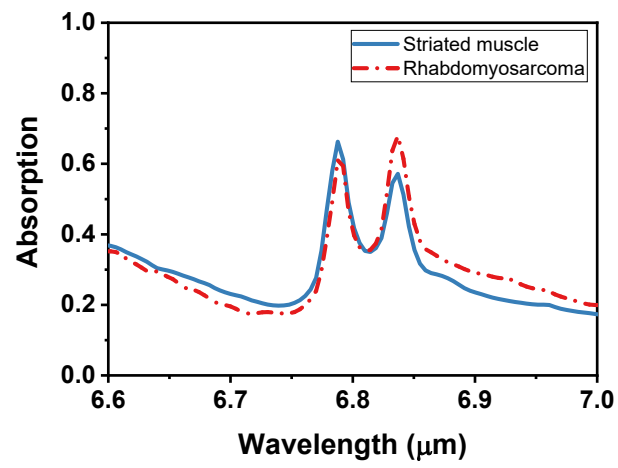


Fig.S7 Absorption spectra of striated muscle and rhabdomyosarcoma tissue under unpolarized conditions.